SCIENTIFIC REPORTS

OPEN

SUBJECT AREAS:
STRESS SIGNALLING
APOPTOSIS
REPROGRAMMING
CELL PROLIFERATION

Received
6 March 2013

Accepted
10 June 2013

Published
27 June 2013

Correspondence and requests for materials should be addressed to S.V. (vriz@univ-paris-diderot.fr)

* These authors contributed equally to this work.

† Current address: Department of Molecular, Cellular, and Developmental Biology Yale University- New Haven, CT, USA.

Sustained production of ROS triggers compensatory proliferation and is required for regeneration to proceed

Carole Gauron[2]*, Christine Rampon[1,2]*, Mohamed Bouzaffour[1]†, Eliane Ipendey[2,3], Jérémie Teillon[2], Michel Volovitch[2,3] & Sophie Vriz[1,2]

[1]Université Paris Diderot, Sorbonne Paris Cité. Paris - France, [2]Centre Interdisciplinaire de Recherche en biologie (CIRB) CNRS UMR 7241/INSERM U1050/Collège de France. Paris - France, [3]Department of Biology - Ecole Normale Supérieure. Paris – France.

A major issue in regenerative medicine is the role of injury in promoting cell plasticity. Here we explore the function of reactive oxygen species (ROS) induced through lesions in adult zebrafish. We show that ROS production, following adult fin amputation, is tightly regulated in time and space for at least 24 hours, whereas ROS production remains transient (2 hours) in mere wound healing. In regenerative tissue, ROS signaling triggers two distinct parallel pathways: one pathway is responsible for apoptosis, and the other pathway is responsible for JNK activation. Both events are involved in the compensatory proliferation of stump epidermal cells and are necessary for the progression of regeneration. Both events impact the Wnt, SDF1 and IGF pathways, while apoptosis only impacts progenitor marker expression. These results implicate oxidative stress in regeneration and provide new insights into the differences between healing and regeneration.

The ability to regenerate amputated or injured body parts varies greatly from one species to another. In vertebrates, only teleost fish and amphibian urodeles retain this capability throughout their lifespan[1–3]. The regeneration of complex structures involves the coordinated renewal of many cell types from a small group of cells[1,2,4]. Following amputation, the cells of different lineages from the stump respond to the injury through dedifferentiation into lineage-restricted progenitors that proliferate and accumulate at the damaged surface underneath the wound epithelium, forming a mass of proliferating cells, called the blastema[1,5–9]. During adult caudal-fin regeneration, the scenario for blastema formation has been carefully described and includes several steps[10]. First, connective tissue is sealed with a clot, in which the lateral epidermis migrates to cover the wound. After 15 hours post amputation (hpa), proliferation initiates at the level of the stump epidermis, and after 24–30 hpa, mesenchymal cells undergo mitotic division and begin to migrate distally toward the wound epidermis to form the blastema. At 48 hpa, the blastema is clearly formed[10,11], and a morphogenetic field is established, initiating complex signaling networks that further regulate proliferation and patterning[1,12]. At earlier stages, knowledge at the molecular level primarily concerns the wound epithelium, and at later stages its interaction with blastemal cells[13]. However, the nature of the signals involved in the induction of the early steps of regeneration and their differences in wound healing remain unknown.

Wounds generate reactive oxygen species (ROS), specifically hydrogen peroxide (H_2O_2)[14]. Despite their toxic potential, ROS play important roles as signaling molecules that regulate a broad range of biological processes[15–17]. H_2O_2, a relatively long-lived ROS, is freely diffusible between cells and is a potential signaling molecule in early events after injury. Recently, the Amaya group showed that increased production of ROS plays a critical role in Xenopus tadpole tail regeneration[18]. In the present study, we investigated the function of ROS in blastema formation in adult fish. We show that ROS accumulated at the surface of the lesion immediately after amputation, and more interestingly, ROS are subject to regulation in time and space during the first 24 hours after amputation. We showed that the sustained production of ROS is an essential signal for blastema formation and is specific to regeneration, as it is never observed during wounding. We provided evidence that parallel to apoptosis induction, ROS induces JNK signaling. Both apoptosis and JNK signaling converge in epidermal cell proliferation at 24 hpa and are essential for blastema formation.

Results

Sustained production of ROS after amputation. As a first step to examine the role of ROS in regeneration, we characterized ROS production during wounding and fin regeneration. Injury-induced ROS production was

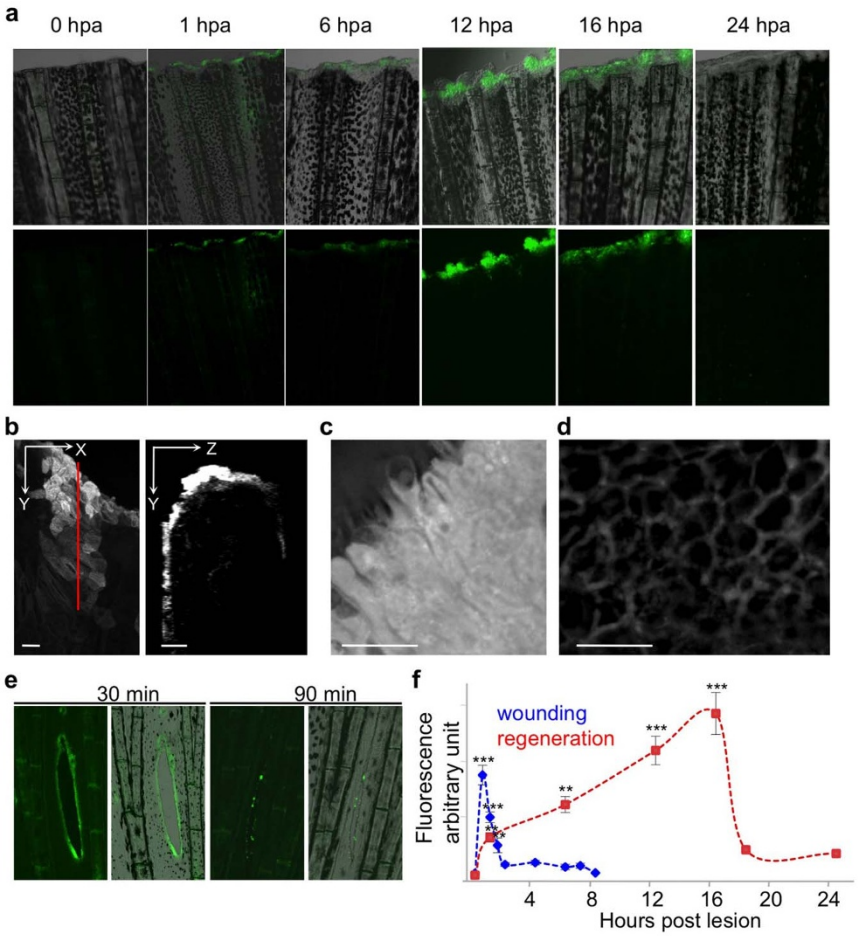

Figure 1 | Sustained production of ROS is specific to regeneration. (a–e) ROS were detected with a fluorescent probe (H_2DCFDA) in the time course of regeneration (a–d) or during wounding (e). (a) Top row: merge; bottom row: ROS detection. (b) At 16 hpa and higher magnification, orthogonal projection showed that ROS were primarily detected in the epidermis. (c–d) At 16 hpa, ROS were abundant in the wounded epidermis (c) and decorated adjacent epidermal cells (d). (e) Left panel: ROS detection; right panel: merge. (f) Quantification of the amount of ROS during healing and regeneration. Error bars represent the SEM (**p< 0.01, ***p < 0.001). Scale bars= 20 μm.

detected in live adult zebrafish using a free permeable radical sensor (H_2DCFDA). This non-fluorescent form of fluorescein is converted to the highly fluorescent 2′,7′-dichlorofluorescein (DCF) upon cleavage of the acetate group through oxidation. Anesthetized fish were amputated and fluorescence was monitored through confocal microscopy. After amputation, ROS were detected uniformly at the level of the amputation plane a few minutes after amputation, with detection lasting for several hours (6 hpa) (Fig. 1a, f). Surprisingly, at 12 hpa, ROS were still highly detected at the tip of the amputated fin but almost exclusively at the level of the inter-ray (Fig. 1a and higher magnification in Fig. S1a). At 16 hpa, ROS were observed along the entire tip of the fin (Fig. 1a; Fig. S1a). By 24 hpa, ROS could no longer be detected at the level of amputation plane (Fig. 1a, f) but in isolated cells of the stump (Fig. S1b). To better characterize the localization of ROS, we collected Z-stack images from 16-hpa samples. Orthogonal sections at the level of the amputation plane showed that ROS were detected in the epidermis (Fig. 1b). Higher magnification showed that ROS were strongly released in the wound epidermis (Fig. 1c) and detected at the level of the cytoplasmic membrane in the adjacent stump epidermis (Fig. 1d). The sustained production of ROS was specific to regeneration because the wounding caused by cutting slits in the fin between rays induced ROS production around the lesion with a peak at 30 minutes post lesion and no ROS detection after 2 hours post lesion (hpl) (Fig. 1e, f). Notably, under these conditions, wound closure is complete at 5 hpl and at least 3 hours after the end of ROS detection (Fig. S2). These results indicate that after injury, ROS production depends on the lesion type. ROS is produced for less than 2 hours in the context of wounding, as observed in larva regeneration[14], but ROS was sustained for 18 hours in adult regenerating tissue (Fig. 1f). This result suggests that in adult fish, ROS are produced long after wound closure (10 – 12 hpa) and might participate in blastema formation. To directly examine the role of ROS during regeneration, we used a pharmacological inhibitor of NADPH oxidase (VAS2870) to reduce the production of ROS in the regenerating fin. Continuous treatment of fish with VAS2870, from the time of amputation to 6 hpa, significantly reduces ROS production at 6 hpa (Fig. S1c). This experiment indicated that this inhibitor could be used to reduce ROS production in the regenerating fin.

NOX activity is essential for regeneration to proceed. To directly test the impact of NOX (NADPH oxidases) on regeneration, we quantified the effect of NOX inhibition on the size of the regenerate at 72 hpa. Treatment with VAS2870 or DPI, another NADPH oxidase (NOX) inhibitor, from the time of amputation to 72 hpa, strongly reduced the size of the regenerate at 72 hpa (Fig. 2a). In addition, inhibition of NOX activity from 12 to 24 hpa had a comparable effect on regenerate size (Fig. 2a). It thus appears that NOX activity between 12 to 24 hpa participates in an early signaling pathway involved in the initiation of regeneration (blastema formation). Both DPI and VAS2870 are commonly used to inhibit NOX. VAS2870 is active on all NOX (pan-NOX) and is more specific

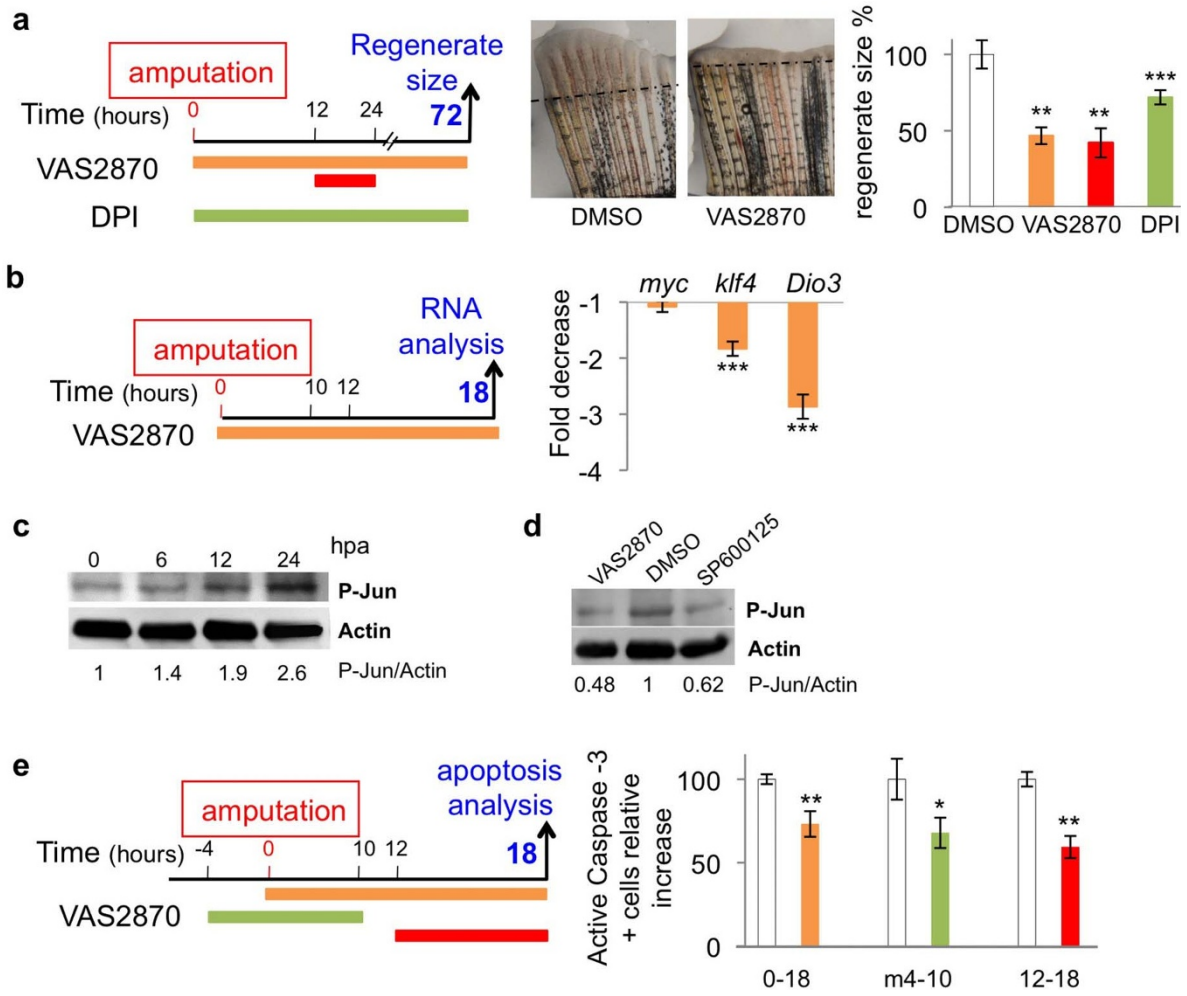

Figure 2 | Sustained ROS production is essential for regeneration to proceed. (a) Inhibition of NADPH oxidase with VAS2870 1 μM or DPI 1 μM reduced the size of the regenerate at 72 hpa. Representative images are shown. The efficiency of regeneration was quantified at 3 dpa (day post amputation). The surface of the blastema was measured and subsequently divided using the square length of the amputation plane for each fish. The efficiency of regeneration is expressed as a percentage of the control. (b) Gene expression was analyzed through quantitative RT-PCR on the regenerated fin at 18 hpa after VAS2870 (1 μM) or vehicle (DMSO) treatment. The DMSO-treated sample was taken as 1. (c, d) Quantification of phospho-c-JUN was performed on western blots. Full-length western blots are presented in Supplementary Figure 5. (d) The inhibition of NADPH oxidases (NOX) with VAS2870 (1 μM) or JNK activity with SP600125 (5 μM) reduced c-Jun phosphorylation at 6 hpa. (e) The inhibition of ROS (VAS2870 1 μM) production decreased apoptosis at 18 hpa. In representative pictures, dotted lines indicate amputation plane. The error bars represent the SEM (* $p<0.05$, ** $p< 0.01$, *** $p < 0.001$).

to NOX than DPI[19]. This is why VAS2870 was used to further analyze NOX activity. To characterize the impact of NOX activity on progenitor cell recruitment, we examined whether NOX inhibition affected cell reprogramming. The expression of stem-cell pluripotency factors has been reported during epimorphic regeneration in the newt[20] and zebrafish[21]. We measured the expression of proto-oncogene *myc-a* (*myc*) and Krüppel-like factor 4 (*klf4*), which are among the first genes to mark the progenitor cell fate. We also analyzed the expression of deiodinase-3 (*dio3*), an enzyme implicated in progenitor cell proliferation[22,23]. NOX inhibition had no effect on myc expression, but reduced the expression of both klf4 and dio3 (Fig. 2b).

Oxidative stress has been implicated in MAP kinase activation and apoptosis[15]. To better characterize the early signals engaged through ROS and relayed into the stump for progenitor cell recruitment, we decided to examine the involvement of ROS in these processes. Junb and junbl have been previously identified as early induced genes during the process of fin regeneration[24,25], and it has been shown that JNK activity is required at early steps of fin regeneration[25]. Indeed, it has been shown that the MAP kinase phosphatases, which dephosphorylate and inactivate JNK, are critical targets of ROS[26]. Oxidation of MKPs leads to inactivation of the phosphatases and thereby serves to sustain JNK activation. Furthermore, it has been recently shown that H_2O_2 is responsible for Src family kinase Lyn induction during wounding in zebrafish larvae[27]. We first confirmed that P-JUN is activated as early as 6 hpa (Fig. 2c), and the pharmacological compound SP600125 inhibited JNK activity in fish (Fig. 2d). We then used the pan NOX inhibitor VAS2870 to determine whether ROS production was involved in JNK activation. Indeed, NOX inhibition led to a reduction (50%) in P-JUN detection (Fig. 2d). We concluded that ROS are involved in JNK activation as early as 6 hpa.

We then examined whether NOX was correlated with apoptosis in the injured fin. For this purpose, fish were incubated in VAS2870 or vehicle, and apoptosis was detected at 18 hpa using an anti-activated caspase-3 antibody (Fig. 2e). The inhibition of ROS production reduced the number of apoptotic cells. Moreover, inhibition of NOX from 12 to 18 hpa was sufficient to reduce the number of apoptotic cells at 18 hpa, suggesting that ROS production during this late period (between 12 and 18 hpa) is involved in delayed apoptosis.

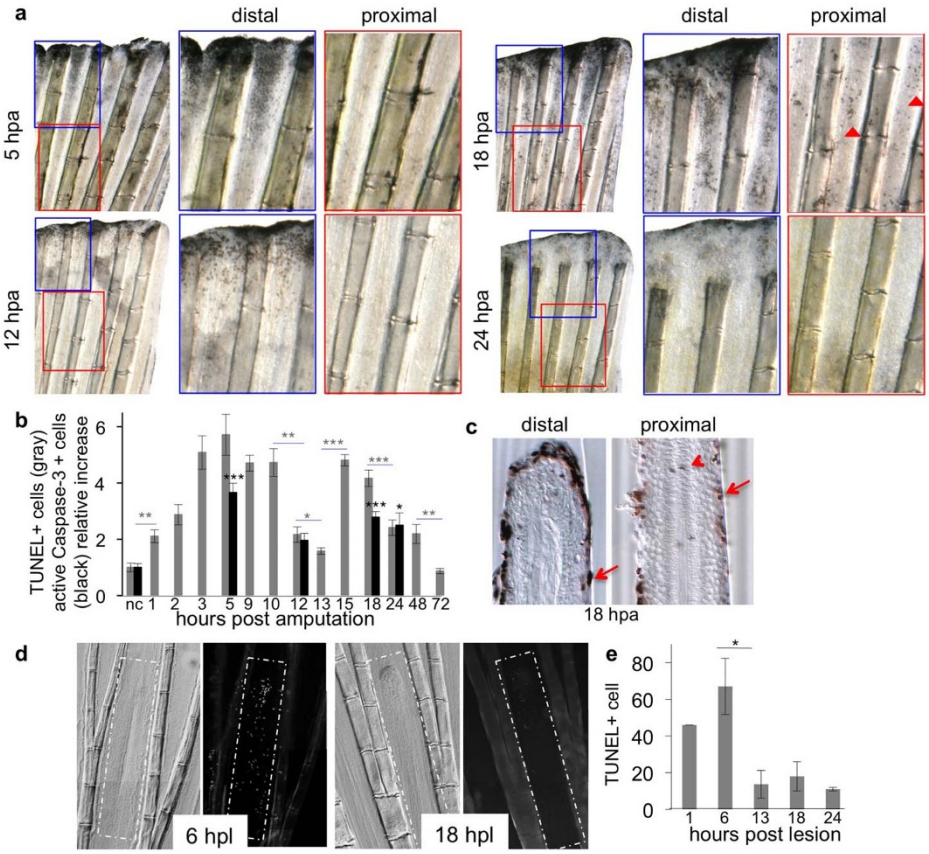

Figure 3 | Spatio-temporal control of cell death during regeneration and wounding (a–c) TUNEL staining during the time course of regeneration. For each time point, a higher magnification is shown for the distal (segment 1 and 2, blue frame) and proximal (segment 3–4, red frame) regions of the fin. Numerous TUNEL-positive cells were detected in the proximal region of the fin (segments 3–6) at 18 hpa (arrowheads). (b) Quantification of cell death. For each fin, TUNEL-positive cells (gray) or active Caspase-3 positive cells (black) were counted in ray and inter-ray 2 in all segments. The uncut control (nc) corresponds to positive cells below the level of amputation in amputated fins (first bifurcation level) and was taken as 1. (c) Longitudinal cross-sections obtained at 18 hpa revealed numerous positive cells in the stump epidermis (arrows) and only a few cells in the mesenchyme (arrowhead). (d, e) Time course of cell death during wounding. TUNEL staining was performed over the indicated time period. The error bars represent the SEM (* $p<0.05$, ** $p< 0.01$, *** $p < 0.001$).

Notably, an equivalent treatment is sufficient to reduce the size of the blastema at 72 hpa (Fig. 2a). This result shows that ROS, in addition to activated JNK in the early step of regeneration, is also involved in apoptosisinduction in the first 18 hours following amputation. Apoptosis had been implicated in regeneration in vertebrate larvae regeneration[28], planarian[29,30] and hydra regeneration[31], but has never been studied in adult regeneration in vertebrates (for review[2,3]). A direct link between apoptosis and regeneration was observed in other systems; therefore, we carefully examined the time course of apoptosis during the process of adult fin regeneration.

Spatio-temporal regulation of cell death and apoptosis. Cell death and apoptosis were detected using a TUNEL assay and anti-active Caspase-3 immunodetection, respectively. We used fish pigmentation mutants (nacre or golden fish) to obtain clearer results (Fig. 3a–c). Within 1 hpa there was a significant increase in TUNEL-positive cells (Fig. 3b). This number increased to 5 times the number in uncut fins at 5 hpa, followed by a reduction in the number of TUNEL-positive cells to twice that of the baseline at 12–13 hpa. During the following 3 hours, the number of TUNEL-positive cells abruptly increased in a second round of cell death at 15–18 hpa, followed by a reduction that reached baseline at 72 hpa. The tissue sections showed that TUNEL-positive cells were concentrated in the stump epidermis, with very few cells observed in the mesenchyme (Fig. 3c; Fig. S3b). The detection of apoptotic cells (active caspase-3 positive cells), rather than necrotic plus apoptotic cells (TUNEL positive cells), displayed the same kinetics (Fig. 3b). Taken together, these results show that cell death is both temporally and spatially regulated in the regenerating fin with significant changes in the stump epidermis. The existence of two rounds of cell death was specific to regeneration, as wounding induced through cutting slits in the fin between rays resulted in cell death around the lesion at 1 hpl and a more widespread distribution of cell death at 6 hpl, followed by a continuous decrease in cell death events (Fig. 3d, e). A second wave of cell death was not observed (Fig. 3e). Notably, in this wounding assay, ROS are produced at the lesion site for no more than 2 hours (Fig. 1f).

At 15 hpa, when we observed strong ROS production and a second round of cell death in the stump epidermis, the mesenchyme under the lesion starts to disorganize up to segment 7 [11], allowing differentiated cells to acquire a proliferative state and migrate toward the forming blastema, corresponding to a progenitor recruitment step. Consequently, cell death in the stump epidermis might contribute to mesenchymal tissue remodeling and blastema formation. We decided to directly examine this hypothesis.

Inhibition of apoptosis impairs blastema formation. To consider the role of apoptosis in cell death during regeneration, we inhibited apoptosis in the regenerating fin. We used NS3694, an inhibitor of apoptosome caspase activation[32], rather than Z-VAD, which is highly toxic in the adult fish (not shown). In the first series of experiments, the fish were treated continuously from the time of amputation until 18 hpa, and cell death was monitored through

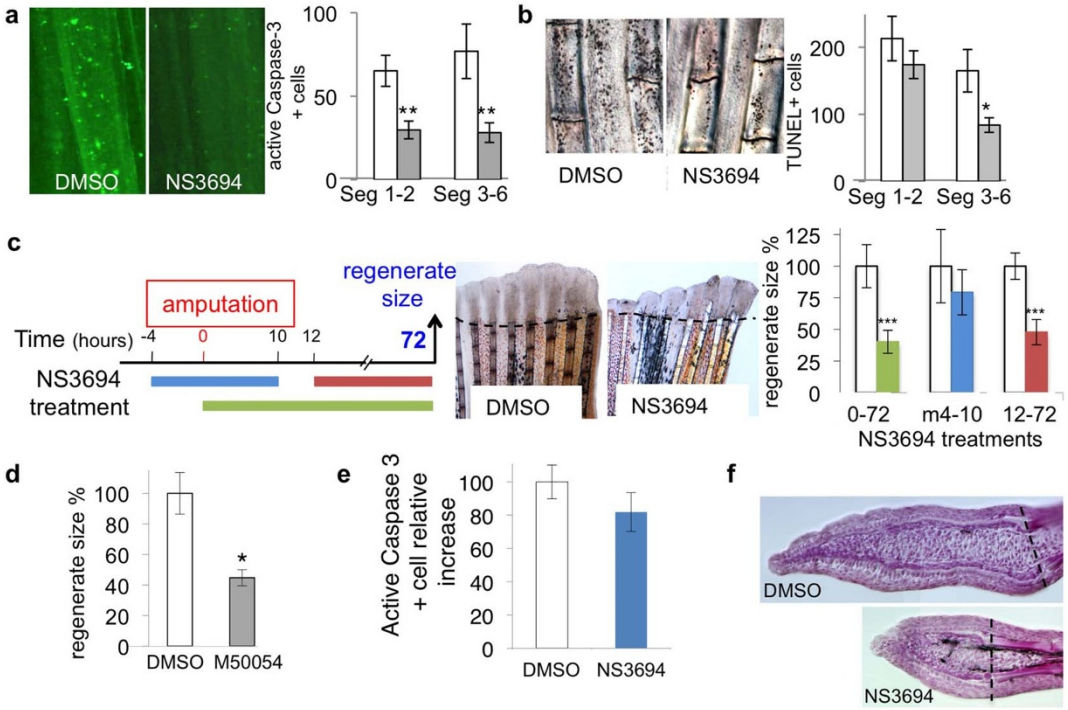

Figure 4 | Inhibition of apoptosis impairs blastema formation. (a, b) TUNEL assay and immuno-detection of active Caspase-3 were performed on 18-hpa samples (white: DMSO; grey: NS3694 5 μM). (c) The efficiency of regeneration was quantified at 72 hpa and is expressed as a percentage of control; representative fins are shown. (d) Fish were incubated in M50054 (a cell permeable inhibitor of apoptosis) at 30 μM or vehicle (DMSO) from the time of amputation to 3 dpa. The efficiency of regeneration was quantified at 3 dpa and is expressed as a percentage of the control. (e) The inhibition of the first wave of apoptosis does not affect the second wave. Fish were incubated in NS3694 (5 μM) or vehicle (DMSO) from 4 hours before amputation to 12 hpa. The fish were subsequently transferred to water until 18 hpa. The fins were collected, and the immuno-detection of active Caspase-3 was performed. Positives cells were counted in ray and inter ray 2 for each fin. No significant differences were observed. (f) Hematoxylin-stained longitudinal sections of the regenerated fin at 3 dpa with or without NS3694 treatment. In representative pictures, the dotted lines indicate amputation plane. The error bars represent the SEM (* $p<0.05$, ** $p< 0.01$, *** $p < 0.001$).

either active caspase-3 immuno-detection or TUNEL assay. Treatment with NS3694 reduced the number of activated caspase-3-labeled cells to 50% in segments adjacent to the lesion as well as in segments further away from the lesion (Fig. 4a). Apoptosis inhibition also led to a strong decrease in TUNEL positive cells in the proximal region of the fin (50% reduction in segments 3–6), however little impact was observed in the distal region (segments 1–2) (Fig. 4b). This indicated that NS3694 was able to inhibit 50% of apoptosis and that apoptosis is the major cause of cell death in the proximal region (Seg 3–6) of the fin at 18 hpa. We then examined the effect of apoptosis inhibition on blastema formation. Treatment with NS3694 from the time of amputation to 72 hpa (condition 0–72) or from 12 to 72 hpa (condition 12–72) strongly inhibited blastema formation, while NS3694 had no effect on regeneration when applied from −4 to 10 hpa (condition m4-10)(Fig. 4c). NS3694 treatment from −4 to 10 hpa had no impact on apoptosis at 18 hpa (Fig. 4e), which confirms that early apoptosis had no effect on regeneration. The impact of apoptosis inhibition on blastema formation was confirmed using another anti-apoptotic drug (M50054) (Fig. 4d). Hematoxylin-staining of longitudinal sections of the 3 dpa regenerate confirmed a reduction in size, but no specific difference was observed in the general organization of the blastema between NS3694 treated and control fins (Fig. 4f). Thus, apoptosis impacts the number of blastemal cells, rather than the structure of the regenerate. To better understand the impact of apoptosis and JNK inhibition on blastema formation we used three additional readouts: 1) proliferation in the stump epidermis, 2) expression of signaling molecules involved in wound epidermis-blastema cross talk or blastemal cell proliferation, and 3) progenitor cell marker expression at 18 hpa.

JNK and apoptosis are involved in compensatory proliferation. A prominent feature of the first 24 hours following amputation is proliferation in the stump epidermal compartment[10,11], and ROS, JUNK and apoptosis have been implicated in cell proliferation[17]. We thus examined the implication of these signaling pathways in epidermal cell proliferation at 24 hpa. Fish were amputated and incubated in drug or vehicle until 24 hpa. The cells in mitosis were detected through immunochemistry using an anti-H3-P antibody. At 24 hpa, the mitotic cells were not ubiquitously distributed in the epidermis, but mainly localized in the inter-ray epidermis of the stump (Fig. 5a). The inhibition of ROS production with VAS2870, apoptosis with NS3694 and JNK with SP600125 reduced the number of positive cells to half (Fig. 5a). Thus, ROS, apoptosis or JNK signaling are required for epidermal cell proliferation in the stump. In many systems, JNK signaling is involved in apoptosis induction[17]. We therefore assessed the effect of JNK signaling on cell death. After amputation, the fish were incubated in the JNK inhibitor (SP600125) or vehicle and TUNEL-positive cells scored at 18 hpa (Fig. 5b). Surprisingly, the inhibition of JNK had no effect on the number of dying cells (Fig. 5b), suggesting that in this system, JNK is not involved in the induction of apoptosis. As both apoptosis and JNK activation are involved in epidermal cell proliferation at 24 hpa, we concluded that these two signaling pathways work in parallel with each other and downstream of ROS.

Apoptosis but not JNK is required for pluripotency marker expression. Finally, to further characterize the effect of apoptosis/JNK signaling, we examined whether their inhibition affected cell reprogramming, similar to NOX inhibition. After amputation, the

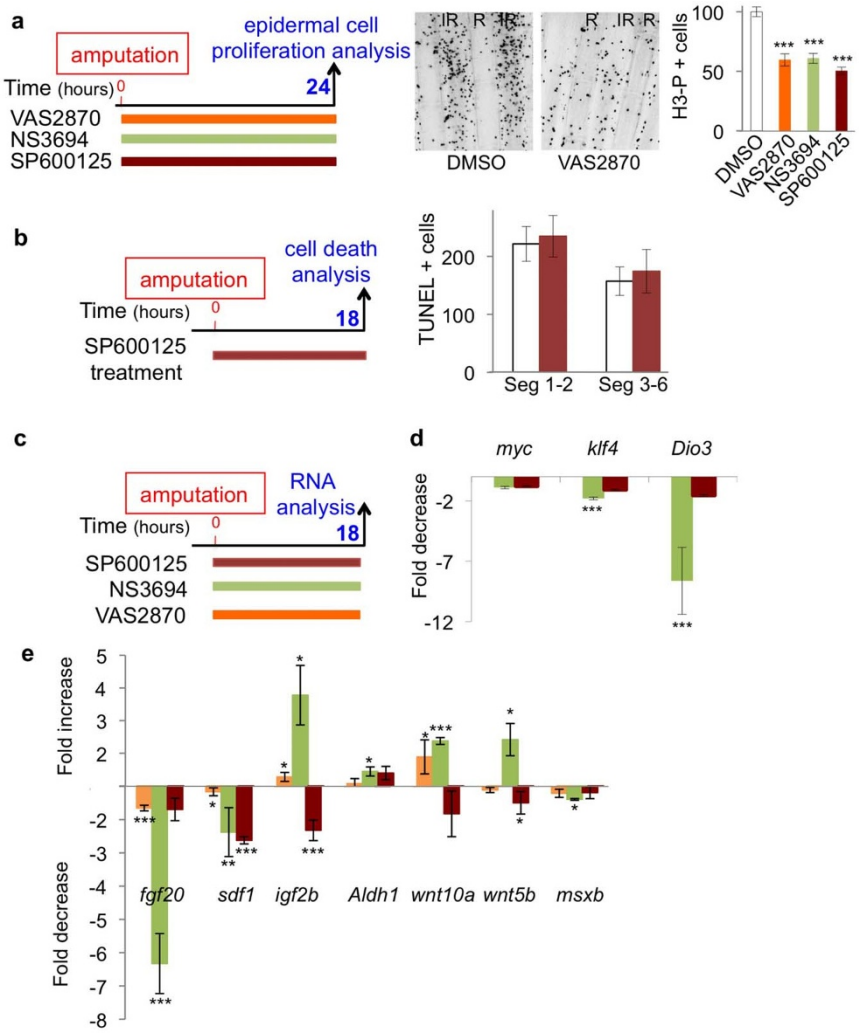

Figure 5 | JNK and apoptosis are involved in compensatory proliferation. (a) Inhibition of ROS production (VAS2870 1 μM), Apoptosis (NS3496 5 μM) and JNK (SP600125 5 μM) reduced the number of epidermal cells in mitosis at 24 hpa. Proliferation in the epidermis was monitored through the phosphorylated histone H3 (H3-P). Representative pictures are shown. H3-P positive cells were counted in rays and inter-rays-2 from segment 1 to segment 6 at 24 hpa. (b) Inhibition of JNK (SP600125 5 μM) had no effect on cell death at 18 hpa. (c–e) Gene expression was analyzed through quantitative RT-PCR on the regenerated fin at 18 hpa after NS3694 (5 μM), (SP600125 5 μM), VAS2870 (1 μM) or vehicle (DMSO) treatment. The DMSO-treated sample was taken as 1. The error bars represent the SEM (* $p<0.05$, ** $p< 0.01$, *** $p < 0.001$).

fish were treated with NS3694 or SP600125 and the amount of mRNA was analyzed at 18 hpa by QRT-PCR (Fig. 5c, d). Continuous inhibition of apoptosis for 18 hpa had no effect on the *myc* mRNA level. In contrast, the same treatment clearly affected *klf4* (reduced by a factor 2) and *D3* (reduced by a factor greater than 8) mRNA. A reduction was also observed when NS3694 was applied only between 10 and 18 hpa (second round of apoptosis), whereas the same treatment was inefficient when applied between -4 and 6 hpa (Fig. S4). Unlike apoptosis inhibition, JNK inhibition had no effect on *klf4* and *dio3* expression (Fig. 5c–d). Thus, the second round of apoptosis affects blastema formation via cellular reprogramming, but not JNK. As both treatments lead to an inhibition of the regenerate size, we examined the impact of apoptosis and JNK inhibition on the expression of signaling molecules involved in blastema growth (Fig. 5c, e). It has been proposed that cross talk between the wound epidermis and blastema involves several diffusible molecules, such as Igf2b[33], Sdf1[34,35], Fgf20[36], Wnt[37] and retinoic acid (aldh1a2)[38]. We thus examined the impact of NOX, apoptosis and JNK inhibition on the expression of these genes. After amputation, the fish were treated with VAS2870, NS3694 or JNK inhibitor, and the amount of mRNA was analyzed at 18 hpa through QRT-PCR (Fig. 5e). Although a reduction of apoptosis through the inhibition of NOX activity is not complete, impairing NOX activity induces a reduction of fgf20 and sdf1, as well as an enhancement of igf2b and wnt10a similar to that of apoptosis (Figure 5e). It seems that *msxb* was not regulated through these pathways. On the other hand, JNK inhibition significantly reduced the expression of *sdf1, wnt5b* and *igf2b*, but had no significant effect on *fgf20* and *wnt10* expression. This result confirmed that the apoptosis pathway is distinct from the JNK pathway during blastemal cell recruitment.

Discussion

The definition of progenitor cells (origin and maintenance) has evolved in recent years, and re-programming of differentiated cells has become a focus of research. A major issue in regenerative medicine is how to control the cellular environment in order to promote the differentiated/progenitor transition *in vivo*. In this context, amphibian and fish provide relevant models of regeneration for studying the signals required for progenitor recruitment after lesion[3]. Although any differentiated cell can participate in blastema formation[6–9,39,40], only a few cells respond to injury by assuming a progenitor identity, while majority of cells maintain their identity and tissue

structure. We show here that ROS signaling occurs early in this process.

Microarray analysis during Xenopus tropicalis tadpole tail regeneration has revealed an induction of the genes governing the NADPH metabolic pathway shortly after amputation and points toward ROS production as a potential important feature in regeneration[41]. More recently, the same group demonstrated that injury-induced ROS production is an important regulator in Xenopus tadpole regeneration[18]. It has been shown that H_2O_2 is produced shortly after tail amputation in zebrafish larvae, peaking at 20 min after lesion and that this signal is responsible for leukocyte recruitment to the wound[14] and sensory axon regeneration[42]. Recently, these results were confirmed through the observation that a redox sensor in leukocytes, which detects H_2O_2 at the wounds in zebrafish larvae (Fyn, a Src family kinase member), is essential for larval regeneration[27]. We showed that, in the context of adult regeneration, ROS production is not restricted to early wound healing, but is sustained for several hours after lesion and initiates several signaling pathways. It has recently been proposed that ROS signaling is concentration dependent and that, whereas high ROS levels induce cell death, moderate levels of ROS could activate the inflammatory response and low levels of ROS activate metabolic signaling[43]. We hypothesize that in the adult fin, amputation induces ROS production, which in turn establishes at least two independent pathways, apoptosis and JNK, for epidermal cell proliferation.

We demonstrated that the first wave of apoptosis does not interfere with the second wave and that the second wave is essential for regeneration. In addition, we showed that ROS are responsible for this second wave of apoptosis. We have no direct molecular cues for the link between ROS production and apoptosis, but it is interesting to note that amputation induces a transcutaneous voltage essential for blastema formation[1,44], and voltage-gated potassium channels (Kv channels) regulate apoptosis[45] and are directly activated through NADPH oxidase-derived ROS in animals[46] and plants[47].

The peak of ROS production and the second wave of cell death, which is specific and essential for regeneration to proceed, both occur around 15 hpa, which correlates with proliferation in the stump epidermis compartment and blastemal cell recruitment[10,11]. Previous work has associated the inhibition of proliferation in the stump epidermis with blastema formation failures[34]. The first consequence of inhibiting apoptosis and JNK signaling is a strong reduction in epidermal cell proliferation. This result suggests that proliferation in the stump epidermis corresponds to a compensatory event, induced through apoptosis and the JNK pathway. The promotion of cell division through apoptotic cells has been well documented in recent years and can now be considered as a key element in tissue homeostasis[48].

The second impact of inhibiting apoptosis/JNK signaling is a reduction of the size of the blastema. At this stage, the potential link between the two phenomena remains elusive, and as yet, no direct link has been drawn between proliferation in the stump epidermis and blastemal cell recruitment. The direct effect of epidermal cell proliferation on blastemal cell recruitment presumes a long range signaling mechanism. This could be achieved by through mechanical forces induced by epithelium deformation[49]. The concept of "mechano-niche" has recently been proposed[50], and studies on the response of stem or progenitor cells to mechanical forces have recently flourished[51]. However, the design of conclusive experiments in adult fish remains difficult.

In conclusion, we identified the sustained production of ROS at the level of the amputation plane, as an early, essential and specific event in the path from lesion to progenitor cell recruitment (Fig. 6). This result indicates the potential of screening for cellular and molecular cues that discriminate wound healing from regeneration as early as 12 hours after amputation. We showed that in the path from lesion to progenitor cell recruitment, ROS signaling was relayed, at least in part, through proliferation and apoptosis that occurred in the stump epidermis, far from the amputation plane. ROS are highly diffusible molecules and future experiments are needed to explain the preferred signaling propagation in the inter ray epidermis, rather than that in rays. Finally, we provide evidence that apoptosis downstream of ROS is essential for progenitor cell recruitment. Deciphering the signals engaged by apoptotic cells would help to understand which pathways are important to modify cell identity in mature tissue and to push them to acquire a progenitor phenotype. This knowledge will be of importance to manipulate regenerative capacities in mammals.

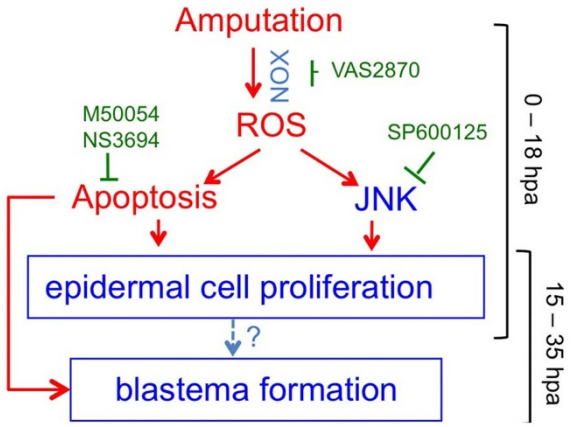

Figure 6 | Schematic representation of early events following amputation. Amputation triggers a sustained ROS production that induces apoptosis and JNK signaling. Both signaling pathways are important for epidermal cell proliferation at 24 hpa and are necessary for blastema formation. ROS through Apoptosis signaling stimulates pluripotency marker expression.

Methods

Fish care, surgery and quantification of regeneration. Zebrafish colonies (AB-Tu, nacre and golden fish) were maintained using standard methods. The animal facility obtained a French agreement from the ministry of agriculture for all the experiments performed in this manuscript (agreement n° B 75-05-12) and protocols has been approved through the Collège de France ethic committee. For manipulation and amputation, adult zebrafish (5–10 months of age) were anesthetized in 0.1% tricaine (ethyl-m-aminobenzoate), the caudal fins were amputated at the level of the first ray bifurcation, and the fins were allowed to regenerate for various lengths of time. The fish were subsequently anesthetized, and the regenerating fins were collected for further analysis. The efficiency of regeneration was quantified at 3 dpa (days post amputation). The surface of the blastema was measured and subsequently divided using the square length of the amputation plane for each fish. The efficiency of regeneration is expressed as a percentage of the control. For wounding assay, fish were anesthetized, and the fins were cut (2 to 3 segments long) between rays 2 and 3 at the level of the first ray bifurcation.

Reactive oxygen species (ROS) detection. The compound 2′,7′-dichlorofluorescin diacetate (H_2DCFDA, Calbiochem) was used to monitor the accumulation of reactive oxygen species in adult zebrafish fin. Fluorescent DCF was formed through ROS oxidation. Zebrafish were incubated with H_2DCFDA (50 μM) at 2 hrs prior to confocal imaging. Spinning-disk images were acquired using a 4×/0.15 N.A. objective on a Nikon Eclipse Ti microscope, equipped with a CoolSnap HQ2/CCD-camera (Princeton Instruments) and a CSUX1-A1 (Yokogawa) confocal scanner. MetaMorph software (Molecular Devices) was used to collect the data. Fluorescence was excited with a 491 nm laser and detected with a 525/39 nm filter. The z-stack acquisition (Fig. 1b) were acquired using an inverted Leica SP5 with a Leica PL APO 20x/NA=0.7 oil immersion objective. The distance between each plane is 1.7 μm. Fluorescence was excited with a 488 nm laser and detected from 500 to 550 nm. Quantification of fluorescence intensity and orthogonal projection were performed using ImageJ software.

Detection of cell death. The fins were fixed in 4% paraformaldehyde overnight at 4°C, and an *In situ* Cell Death Detection Kit (Roche) was used for TUNEL assays on whole fins or cryosections. For each fin, the positive cells were counted in ray and inter-ray 2 in all segments. After TUNEL assay on whole fins, the fins were embedded as previously described[34] and sections (20 μm) were cut using a vibratome to analyze the localization of positive cells. Alternatively, cell death was detected on cryosections.

For cryosectioning, the following protocol (http://www.nd.edu/~hydelab/protocols/general/IF_protocol.html) was followed using Roche's recommendations for TUNEL detection on sections. The images were obtained using an Nikon 90i camera.

Drug treatments. A maximum of five fish were incubated in 200 ml of water for all pharmaceutical treatments. VAS-2870 was purchased from Enzo Life Sciences (# BML-El395-0010). Diphenyleneiodonium chloride (DPI) (# D2926) and SP600125 (#S5567) were obtained from Sigma. NS3694 (# 178494) and M50054 (# 178488) were purchased from Calbiochem. For all drugs, a stock solution was prepared in DMSO. When DPI or NS3694 were used, the fish were maintained in the dark and returned to the light for 1 h per day for feeding and water change. Fish incubated in DMSO comprised the control group.

Immunohistochemistry. The fins were fixed in 4% paraformaldehyde overnight at 4°C and used for whole-mount immunohistochemistry with anti-phospho-histone H3 (SC-8656-R, Santa Cruz) to detect proliferative cells, anti-active Caspase-3 antibody (ab13847, Abcam) to detect apoptotic cells. For each fin, the positive cells were counted in ray and inter-ray 2 in all segments. Images were obtained using a Nikon spinning-disk Roper microscope operated with Metamorph premier 7.6 software or a Nikon 90i camera.

Quantitative RT-PCR. cDNA synthesis and QRT-PCR were performed as previously described[35]. Gene expression levels were normalized to *Rpl13a*[52]. Each sample was tested in triplicate for SYBR Green assays, and in duplicate for Taq Man assays. Quantitative PCR was performed using Light Cycler 480 detection system (Roche) and, either Sybr Green® labeling system (Roche), or Taq Man® methodology using a fluorescent probe-PCR (FAM-NFQ/MGB) (Applied Biosystems). Primers and probes for TaqMan® assays come from the Applied Biosystems bank (Assays ID: rpl13: Dr03119261_m1; klf4: Dr03080183_m1; Dio3: custom assay AJ20SMU). For SYBR Green assay, the *Rpl13a* primers were previously described in[52], *igf2b*[33], *fgf20a* in[35], *D3* in[23] and *myc-a* and *klf4* in[21], *wnt10a, wnt5b, aldh1a2, wnt10b* in[38]. The *sdf1a* primers were fw: 5′-GTCAACACAGTCCCACAGAGAA-3′ and rev: 5′-CACACCTCCTTGTTGTTCTTCA-3′. The run protocols were performed according to the manufacturer's recommendations.

Hematoxylin staining. Fins were fixed in 4% PFA in PBS, transferred to methanol and stored at –20°C. The fins were rehydrated prior to cryosectioning. The sections were stained in Mayer's Hematoxylin Solution (Sigma) for 3–5 minutes, washed in water and cleared in 0.37% HCl in 70% ethanol for 5–10 seconds.

Western blot. Proteins were analyzed on NuPage 4–12% Bis-Tris gels (Novex) and subsequently transferred from the gel to Immobilon transfer membrane (Millipore). The residual binding sites were blocked through incubation in TBS containing 0.2% Tween and 5% BSA. The blot was subsequently incubated with anti-Phospho-c-Jun antibody (# 3270, Cell signaling), followed by incubation with the horseradish-peroxidase-conjugated anti-rabbit IgG (#7074S, Cell Signaling). After analysis, the membrane was stripped with Restore Western Blot stripping buffer (Thermo), blocked with TBS containing 0.2% Tween and 5% non-fat milk and incubated with anti-actin-peroxidase antibody (# A3854, Sigma). Immunoreactive proteins were visualized through chemiluminescence (SuperSignal West Femto Maximum Sensitivity substrate, Thermo) with ImageQuant LAS4000 system (GE Healthcare).

Statistical analysis. Continuous variables are expressed as the means ± Standard Error of Mean (SEM). These variables were compared using one-way analysis of variance and the means comparison was performed using Student's t-tests adjusted to a level of 0.05. All statistical tests were two-tailed, and p values <0.05 were considered statistically significant.

1. Brockes, J. P. & Kumar, A. Comparative aspects of animal regeneration. *Annu Rev Cell Dev Biol* **24**, 525–549 (2008).
2. Galliot, B. & Ghila, L. Cell plasticity in homeostasis and regeneration. *Mol Reprod Dev* **77**, 837–855 (2010).
3. Poss, K. D. Advances in understanding tissue regenerative capacity and mechanisms in animals. *Nat Rev Genet* **11**, 710–722 (2010).
4. Nakatani, Y., Kawakami, A. & Kudo, A. Cellular and molecular processes of regeneration, with special emphasis on fish fins. *Dev Growth Differ* **49**, 145–154 (2007).
5. Brockes, J. P. Amphibian limb regeneration: rebuilding a complex structure. *Science* **276**, 81–87 (1997).
6. Kragl, M. *et al.* Cells keep a memory of their tissue origin during axolotl limb regeneration. *Nature* **460**, 60–65 (2009).
7. Knopf, F. *et al.* Bone regenerates via dedifferentiation of osteoblasts in the zebrafish fin. *Dev Cell* **20**, 713–724 (2011).
8. Tu, S. & Johnson, S. L. Fate restriction in the growing and regenerating zebrafish fin. *Dev Cell* **20**, 725–732 (2011).
9. Sousa, S. *et al.* Differentiated skeletal cells contribute to blastema formation during zebrafish fin regeneration. *Development* **138**, 3897–3905 (2011).
10. Santos-Ruiz, L., Santamaria, J. A., Ruiz-Sanchez, J. & Becerra, J. Cell proliferation during blastema formation in the regenerating teleost fin. *Dev Dyn* **223**, 262–272 (2002).
11. Poleo, G., Brown, C. W., Laforest, L. & Akimenko, M. A. Cell proliferation and movement during early fin regeneration in zebrafish. *Dev Dyn* **221**, 380–390 (2001).
12. Stoick-Cooper, C. L., Moon, R. T. & Weidinger, G. Advances in signaling in vertebrate regeneration as a prelude to regenerative medicine. *Genes Dev* **21**, 1292–1315 (2007).
13. Yoshinari, N. & Kawakami, A. Mature and juvenile tissue models of regeneration in small fish species. *Biol Bull* **221**, 62–78 (2011).
14. Niethammer, P., Grabher, C., Look, A. T. & Mitchison, T. J. A tissue-scale gradient of hydrogen peroxide mediates rapid wound detection in zebrafish. *Nature* **459**, 996–999 (2009).
15. Finkel, T. Signal transduction by reactive oxygen species. *J Cell Biol* **194**, 7–15 (2011).
16. Jiang, F., Zhang, Y. & Dusting, G. J. NADPH oxidase-mediated redox signaling: roles in cellular stress response, stress tolerance, and tissue repair. *Pharmacol Rev* **63**, 218–242 (2011).
17. Ray, P. D., Huang, B. W. & Tsuji, Y. Reactive oxygen species (ROS) homeostasis and redox regulation in cellular signaling. *Cell Signal* **24**, 981–990 (2012).
18. Love, N. R. *et al.* Amputation-induced reactive oxygen species are required for successful Xenopus tadpole tail regeneration. *Nat Cell Biol* **15**, 222–228 (2013).
19. Altenhofer, S. *et al.* The NOX toolbox: validating the role of NADPH oxidases in physiology and disease. *Cell Mol Life Sci* **69**, 2327–2343 (2012).
20. Maki, N. *et al.* Expression of stem cell pluripotency factors during regeneration in newts. *Dev Dyn* **238**, 1613–1616 (2009).
21. Christen, B., Robles, V., Raya, M., Paramonov, I. & Belmonte, J. C. Regeneration and reprogramming compared. *BMC Biol* **8**, 5 (2010).
22. Kester, M. H. *et al.* Large induction of type III deiodinase expression after partial hepatectomy in the regenerating mouse and rat liver. *Endocrinology* **150**, 540–545 (2009).
23. Bouzaffour, M., Rampon, C., Ramauge, M., Courtin, F. & Vriz, S. Implication of type 3 deiodinase induction in zebrafish fin regeneration. *Gen Comp Endocrinol* **168**, 88–94 (2010).
24. Yoshinari, N., Ishida, T., Kudo, A. & Kawakami, A. Gene expression and functional analysis of zebrafish larval fin fold regeneration. *Dev Biol* **325**, 71–81 (2009).
25. Ishida, T., Nakajima, T., Kudo, A. & Kawakami, A. Phosphorylation of Junb family proteins by the Jun N-terminal kinase supports tissue regeneration in zebrafish. *Dev Biol* **340**, 468–479 (2010).
26. Kamata, H. *et al.* Reactive oxygen species promote TNFalpha-induced death and sustained JNK activation by inhibiting MAP kinase phosphatases. *Cell* **120**, 649–661 (2005).
27. Yoo, S. K., Freisinger, C. M., Lebert, D. C. & Huttenlocher, A. Early redox, Src family kinase, and calcium signaling integrate wound responses and tissue regeneration in zebrafish. *J Cell Biol* **199**, 225–234 (2012).
28. Tseng, A. S., Adams, D. S., Qiu, D., Koustubhan, P. & Levin, M. Apoptosis is required during early stages of tail regeneration in Xenopus laevis. *Dev Biol* **301**, 62–69 (2007).
29. Hwang, J. S., Kobayashi, C., Agata, K., Ikeo, K. & Gojobori, T. Detection of apoptosis during planarian regeneration by the expression of apoptosis-related genes and TUNEL assay. *Gene* **333**, 15–25 (2004).
30. Pellettieri, J. *et al.* Cell death and tissue remodeling in planarian regeneration. *Dev Biol* **338**, 76–85 (2010).
31. Chera, S. *et al.* Apoptotic cells provide an unexpected source of Wnt3 signaling to drive hydra head regeneration. *Dev Cell* **17**, 279–289 (2009).
32. Lademann, U. *et al.* Diarylurea compounds inhibit caspase activation by preventing the formation of the active 700-kilodalton apoptosome complex. *Mol Cell Biol* **23**, 7829–7837 (2003).
33. Chablais, F. & Jazwinska, A. IGF signaling between blastema and wound epidermis is required for fin regeneration. *Development* **137**, 871–879 (2010).
34. Dufourcq, P. & Vriz, S. The chemokine SDF-1 regulates blastema formation during zebrafish fin regeneration. *Dev Genes Evol* **216**, 635–639 (2006).
35. Bouzaffour, M., Dufourcq, P., Lecaudey, V., Haas, P. & Vriz, S. Fgf and Sdf-1 pathways interact during zebrafish fin regeneration. *PLoS One* **4**, e5824 (2009).
36. Whitehead, G. G., Makino, S., Lien, C. L. & Keating, M. T. fgf20 is essential for initiating zebrafish fin regeneration. *Science* **310**, 1957–1960 (2005).
37. Stoick-Cooper, C. L. *et al.* Distinct Wnt signaling pathways have opposing roles in appendage regeneration. *Development* **134**, 479–489 (2007).
38. Blum, N. & Begemann, G. Retinoic acid signaling controls the formation, proliferation and survival of the blastema during adult zebrafish fin regeneration. *Development* **139**, 107–116 (2012).
39. Singh, S. P., Holdway, J. E. & Poss, K. D. Regeneration of amputated zebrafish fin rays from de novo osteoblasts. *Dev Cell* **22**, 879–886 (2012).
40. Stewart, S. & Stankunas, K. Limited dedifferentiation provides replacement tissue during zebrafish fin regeneration. *Dev Biol* **365**, 339–349 (2012).
41. Love, N. R. *et al.* Genome-wide analysis of gene expression during Xenopus tropicalis tadpole tail regeneration. *BMC Dev Biol* **11**, 70 (2011).
42. Rieger, S. & Sagasti, A. Hydrogen peroxide promotes injury-induced peripheral sensory axon regeneration in the zebrafish skin. *PLoS Biol* **9**, e1000621 (2011).
43. Finkel, T. Signal transduction by mitochondrial oxidants. *J Biol Chem* **287**, 4434–4440 (2012).

44. Adams, D. S., Masi, A. & Levin, M. H+ pump-dependent changes in membrane voltage are an early mechanism necessary and sufficient to induce Xenopus tail regeneration. *Development* **134**, 1323–1335 (2007).
45. Szabo, I., Zoratti, M. & Gulbins, E. Contribution of voltage-gated potassium channels to the regulation of apoptosis. *FEBS Lett* **584**, 2049–2056 (2010).
46. Mittal, M. *et al.* Hypoxia induces Kv channel current inhibition by increased NADPH oxidase-derived reactive oxygen species. *Free Radic Biol Med* **52**, 1033–1042 (2012).
47. Garcia-Mata, C. *et al*. A minimal cysteine motif required to activate the SKOR K+ channel of Arabidopsis by the reactive oxygen species H2O2. *J Biol Chem* **285**, 29286–29294 (2010).
48. Fuchs, Y. & Steller, H. Programmed cell death in animal development and disease. *Cell* **147**, 742–758 (2011).
49. Teng, X. & Toyama, Y. Apoptotic force: active mechanical function of cell death during morphogenesis. *Dev Growth Differ* **53**, 269–276 (2011).
50. Lee, D. A., Knight, M. M., Campbell, J. J. & Bader, D. L. Stem cell mechanobiology. *J Cell Biochem* **112**, 1–9 (2011).
51. Sun, Y., Chen, C. S. & Fu, J. Forcing Stem Cells to Behave: A Biophysical Perspective of the Cellular Microenvironment. *Annu Rev Biophys* **41**, 519–542 (2012).
52. Tang, R., Dodd, A., Lai, D., McNabb, W. C. & Love, D. R. Validation of zebrafish (Danio rerio) reference genes for quantitative real-time RT-PCR normalization. *Acta Biochim Biophys Sin (Shanghai)* **39**, 384–390 (2007).

Acknowledgements

The authors would like to thank Alain Prochiantz for helpful discussions and constant support. The authors would also like to thank Elizabeth Di Lullo for carefully reading and commenting on the manuscript.

Author contributions

C.R., M.V. and S.V. designed the experiment. C.G., C.R., M.B., E.I., J.T., S.V. performed the research. S.V. wrote the manuscript. C.R., M.V. and S.V. analyzed the data and edited the manuscript.

Additional information

Competing financial interests: The authors declare no competing financial interests.

How to cite this article: Gauron, C. *et al.* Sustained production of ROS triggers compensatory proliferation and is required for regeneration to proceed. *Sci. Rep.* **3**, 2084; DOI:10.1038/srep02084 (2013).